

Single crystal growth and crystal structure of HgTeO_2FOH —a layered fluorohydroxooxotellurate(IV) stabilized by weak $\text{F} \cdots \text{OH}$ interactions

Matthias Weil*

*Institute for Chemical Technologies and Analytics, Division of Structural Chemistry, Vienna University of Technology,
Getreidemarkt 9/164-SC, A-1060 Vienna, Austria*

Received 24 March 2004; received in revised form 19 May 2004; accepted 24 May 2004

Abstract

Light-yellow crystals of HgTeO_2FOH were obtained under hydrothermal conditions by reacting stoichiometric amounts of TeO_2 and HgO in diluted HF, or alternatively, by dissolution of TeO_2 and $\text{Hg}(\text{NO}_3)_2 \cdot \text{H}_2\text{O}$ in 15 wt.% HF and subsequent slow evaporation of the solution. The crystal structure (space group $Pca2_1$ (#29), $Z = 4$, $a = 7.8960(7)$, $b = 6.7845(6)$, $c = 6.8641(6)$ Å, 1044 structure factors, 56 parameters, $R[F^2 > 2\sigma(F^2)] = 0.0186$, $\text{Goof} = 1.007$) was determined from a single crystal diffractometer data set and is made up from distorted $[\text{Hg}^{\text{II}}\text{O}_4\text{F}_2(\text{OH})]$ polyhedra and $(\text{Te}^{\text{IV}}\text{O}_2\text{F}(\text{OH}))^{2-}$ anions. These main building units form a layered assembly parallel to (0 1 0). Upon heating, HgTeO_2FOH decomposes above 300 °C in a two-step mechanism under formation of the mixed-valent $\alpha\text{-Hg}^{\text{II}}_2\text{Te}^{\text{IV}/\text{VI}}_2\text{O}_7$ and traces of $\text{Hg}^{\text{II}}_2\text{Te}^{\text{VI}}_2\text{O}_5$ in the first step, and of formation of TeO_2 in the second step.

© 2004 Elsevier B.V. All rights reserved.

Keywords: Chemical synthesis; Crystal growth; Crystal structure and symmetry; X-ray diffraction

1. Introduction

Inorganic materials with non-linear optical properties have a growing impact in science and technology. Application of these materials for frequency conversion, as electro-optical and photonic devices, optical switches etc. make the specific syntheses and crystal growth of new compounds challenging, because they have to meet very special criteria (thermal stability, transparency in the spectral range, excellent optical quality etc.) and, most importantly, their crystal structures have to be non-centrosymmetric. Unfortunately, only about 15% of the known inorganic compounds crystallize in non-centrosymmetric structure types, but in certain structural families the absence of a centre of symmetry is more frequently observed. These families include compounds with small asymmetrical ligands like SCN^- and OCN^- , or with cations having lone-pair electrons such as Tl^{I} , Sn^{II} , Pb^{II} , Sb^{III} and Bi^{III} , or oxoanions like $\text{Se}^{\text{IV}}\text{O}_3^{2-}$, $\text{Te}^{\text{IV}}\text{O}_3^{2-}$ and $\text{I}^{\text{V}}\text{O}_3^-$, respectively, which can cause the asymmetry in the structure.

On this account it seemed appropriate to prepare new non-centrosymmetric candidates in the system $\text{Hg}\text{-Te}^{\text{IV}}\text{-O}$ and to determine their crystal structures. In a recent project, two polymorphs of the mixed-valent $\text{Te}^{\text{IV}/\text{VI}}$ compound $\text{Hg}_2\text{Te}_2\text{O}_7$ have been crystallographically fully characterized [1], and one of the polymorphs (the β -modification) is indeed non-centrosymmetric. Another approach for the preparation of related phases is to (partly) replace oxygen with fluorine and to investigate the system $\text{Hg}\text{-Te}^{\text{IV}}\text{-O}\text{-F}\text{-}(\text{H})$ for which no representatives are known up to now. During these examinations the title compound HgTeO_2FOH was obtained, whose preparation, crystal structure and thermal behaviour is reported in this article.

2. Experimental

2.1. Synthesis

Single crystals of HgTeO_2FOH used for structure analysis were obtained under hydrothermal conditions. For that purpose, 0.12 g (0.75 mmol) TeO_2 (Merck, 99.999%) and 0.163 g (0.75 mmol) HgO (Merck, p.A.) were charged in a Teflon inlay with 10 ml capacity which was two-thirds filled

* Tel.: +43-1-58801-17122; fax: +43-1-58801-17199.

E-mail address: mweil@mail.zserv.tuwien.ac.at (M. Weil).

with a 5 wt.% HF solution and then sealed in a steel autoclave. This device was heated up to 220 °C within 12 h, left at that temperature for five days and cooled down to room temperature in the course of 48 h. Besides canary-yellow Hg_3TeO_6 crystals [2], colourless to light yellow plates of the title compound had formed. Single phase HgTeO_2FOH was prepared by dissolution of 0.4 g (2.5 mmol) TeO_2 and 0.86 g (2.5 mmol) $\text{Hg}(\text{NO}_3)_2 \cdot \text{H}_2\text{O}$ (Fluka, p.A.) in 50 ml of a 15 wt.% HF solution (Merck, p.A.). This solution was then allowed to evaporate slowly at room temperature. After five days crystal growth started, and after the period of two more weeks yellow crystals with a plate-like habit and an edge-length of up to 0.3 mm had formed in the clear solution. The crystals were filtered off, washed with ethanol and acetone and dried in a desiccator over CaCl_2 for two days. The obtained crystals are stable under normal laboratory conditions, but darken to a yellow-brownish colour in daylight, which had no influence on the diffraction intensities. The presence of fluorine and OH was determined qualitatively by wet chemical methods and IR spectroscopic investigations, respectively.

Thermoanalytical analyses were performed in an open system under a flowing N_2 atmosphere on a Mettler-Toledo TG50 (35–700 °C, heating rate 5 °C min^{-1} , corundum crucibles) and a DSC 25 system (35–550 °C, heating rate 5 °C min^{-1} , aluminium capsules).

2.2. Data collection and refinement

Single crystal diffraction intensities from a hydrothermally grown crystal were collected using the ω -scan technique with 0.3° rotation width and 30 s exposure time per frame on a SMART three-circle diffractometer (Siemens) equipped with a CCD camera. Three independent sets of 606 frames were measured thus scanning the whole reciprocal sphere. The measured intensities were corrected for Lorentz and polarization effects and an absorption correction was applied using the program HABITUS [3] by minimizing the internal R_i value and optimizing the crystal shape. The so derived habit was the basis of the numerical absorption correction. The crystal structure was solved by direct methods and refined with the SHELX97 program package [4]. In the final least-squares cycles all atoms were refined anisotropically. The H atom was not included in the refinement because no reliable atom position could be found in the difference map. No higher symmetry was suggested by the PLATON program [5], and the Flack parameter [6] clearly indicates the absence of any centre of symmetry.

Further details of data collection and structure refinement are summarized in Table 1. Final atomic coordinates, equivalent isotropic displacement parameters, anisotropic displacement parameters and selected interatomic distances and angles are listed in Tables 2–4. The calculated

Table 1
Crystallographic data and details of data collection, structure solution and refinement

Diffractometer	SMART (Siemens)
Radiation; wavelength λ (Å)	Mo $K\alpha$; 0.71073
Temperature (°C)	22(2)
Crystal dimensions (mm ³)	0.11 × 0.07 × 0.05
Crystal description	Light-yellow plate
Space group	$Pca2_1$ (no. 29)
Formula units	$Z = 4$
Lattice parameters (Å)	$a = 7.8960(7)$ $b = 6.7845(6)$ $c = 6.8641(6)$
Volume (Å ³)	$V = 367.71(6)$
Formula weight (g mol ⁻¹)	396.20
μ (mm ⁻¹)	49.506
X-ray density (g cm ⁻³)	7.157
Range $\theta_{\min} - \theta_{\max}$	3.96 → 30.47
Range h ; k ; l	-11 → 11; -9 → 9; -9 → 9
Structure solution and refinement	SHELX97 [4]
Measured reflections	4132
Independent reflections	1044
Observed reflections ($I > 2\sigma(I)$)	978
R_i	0.0313
Absorption correction	HABITUS [3]
Coefficients of Transmission T_{\min} ; T_{\max}	0.0470; 0.2007
Flack parameter	0.049(9)
Number of parameters	56
Extinction coefficient (SHELXL97)	0.0036(3)
Difference electron density (e Å ⁻³) with distance (Å) to atom	$\Delta\rho_{\max} = 0.97$ (0.45; OH); $\Delta\rho_{\min} = -1.04$ (1.33; F)
$R(F^2 > 2\sigma(F^2))$; $wR(F^2 \text{ all})$	0.0186; 0.0416
Goof	1.007
CSD-number	413078

Table 2
Atomic coordinates and equivalent isotropic displacement parameters (\AA^2)

Atom	Wyckoff position	x	y	z	U_{eq}^a
Hg	4 <i>a</i>	0.16948(3)	0.59541(4)	0.23399(8)	0.01632(9)
Te	4 <i>a</i>	0.07746(5)	0.15284(6)	0.02773(7)	0.01030(10)
O1	4 <i>a</i>	0.1594(7)	0.4111(7)	−0.0003(10)	0.0194(12)
O2	4 <i>a</i>	0.6480(6)	0.2102(9)	0.4633(8)	0.0163(11)
F	4 <i>a</i>	0.0143(7)	0.2313(8)	0.2969(6)	0.0253(11)
OH	4 <i>a</i>	0.3818(6)	0.1497(6)	0.2327(9)	0.0119(9)

$$^a U_{\text{eq}} = (1/3)\sum_i \sum_j U_{ij}a_i^*a_j^* \mathbf{a}_i \cdot \mathbf{a}_j.$$

Table 3
Anisotropic displacement parameters (\AA^2)

Atom	U_{11}	U_{22}	U_{33}	U_{23}	U_{13}	U_{12}
Hg	0.01919(14)	0.01453(14)	0.01525(13)	−0.00400(13)	0.00118(14)	0.00067(9)
Te	0.01061(18)	0.00825(19)	0.01206(18)	0.00005(19)	−0.00006(17)	0.00076(15)
O1	0.027(3)	0.010(3)	0.021(3)	−0.001(2)	0.000(2)	−0.0088(18)
O2	0.008(2)	0.018(3)	0.022(3)	0.012(2)	−0.001(2)	0.001(2)
F	0.032(3)	0.025(3)	0.019(2)	−0.0072(19)	0.009(2)	−0.012(2)
OH	0.011(2)	0.016(2)	0.0093(19)	−0.001(3)	−0.002(2)	0.0040(16)

Table 4
Selected distances (\AA) and angles ($^\circ$)

Hg–O1	2.039(6)	Te–O2#6	1.875(5)
Hg–O2#1	2.061(5)	Te–O1	1.878(5)
Hg–O1#2	2.592(6)	Te–F	1.987(4)
Hg–O2#3	2.696(6)	Te–OH#6	2.051(6)
Hg–F	2.791(5)	Te–OH	2.785(5)
Hg–OH#1	2.855(5)	Te–OH#7	2.929(5)
Hg–F#4	2.997(6)		
Hg–O1#5	3.174(6)	F–OH#7	2.823(6)
Hg–Te#5	3.2840(6)		
O1–Hg–O2#1	172.7(2)	O2#6–Te–O1	96.3(2)
		O2#6–Te–F	85.7(2)
		O1–Te–F	86.1(2)
		O2#6–Te–OH#6	85.3(2)
		O1–Te–OH#6	81.6(2)
		F–Te–OH#6	163.9(2)

Symmetry transformations used to generate equivalent atoms – #1: $x - 1/2, -y + 1, z$; #2: $-x + 1/2, y, z + 1/2$; #3: $-x + 1, -y + 1, z - 1/2$; #4: $x + 1/2, -y + 1, z$; #5: $-x, -y + 1, z + 1/2$; #6: $-x + 1/2, y, z - 1/2$; #7: $x - 1/2, -y, z$.

bond-valence sums [7], using the parameters provided by Brese and O’Keeffe [8], are given in Table 5. Additional crystallographic information on HgTeO₂FOH is available from the Fachinformationszentrum Karlsruhe, D-76344 Eggenstein-Leopoldshafen, Germany, email: crysdata@fiz-karlsruhe.de, by quoting the literature citation, the name of the author and the depository number listed at the end of Table 1. Drawing of structural details were produced using the program ATOMS [9].

3. Results and discussion

HgTeO₂FOH crystallizes in a non-centrosymmetric structure and is the first fluorohydroxooxotellurate(IV)

Table 5
Bond valence analysis (v.u.)^a

	Hg	Te	Σ	Expected
O1	0.834 0.187	1.307	2.328	2
O2	0.786 0.141	1.317	2.244	2
OH	0.092	0.819 (0.112) (0.076)	0.911 (1.099)	2 (including the H atom)
F	0.066 0.038	0.940	1.044	1
Σ	2.144	4.383 (4.571)		
Expected	2	4		

^a Additional contributions resulting from weak bonding interactions are given in brackets.

of this formula type as well as the first member of this structural family with mercury as a cation reported so far. Other crystallographically well-characterized representatives include H₂Te₂O₃F₄ [10,11], (NH₄)TeO(OH)F₂ [11], MTe(OH)F₄ (*M* = K, Rb) [12], as well as the double-salts Na₂Te(OH)F₃(SO₄) and (NH₄)₂Te(OH)F₃(SO₄) [13]. Further known structures are the related fluorooxotellurate(IV) KTeOF₃ [11], and the tellurium(IV) oxidefluorides Te₂O₃F₂ [14] and TeOF₂ [15].

The crystal structure of the title compound consists of distorted [Hg^{II}O₄F₂OH] polyhedra and (Te^{IV}O₂FOH)^{2−} anions as the main building units. Like in many other mercury(II) compounds, the Hg atom shows an explicit two-coordination and is surrounded by two tightly bonded oxygen atoms with almost collinear bonds ($d(\text{Hg}-\text{O})_{\text{short}} = 2.05 \text{ \AA}$, $\angle(\text{O}-\text{Hg}-\text{O}) = 172.7(2)^\circ$). Two remote oxygen

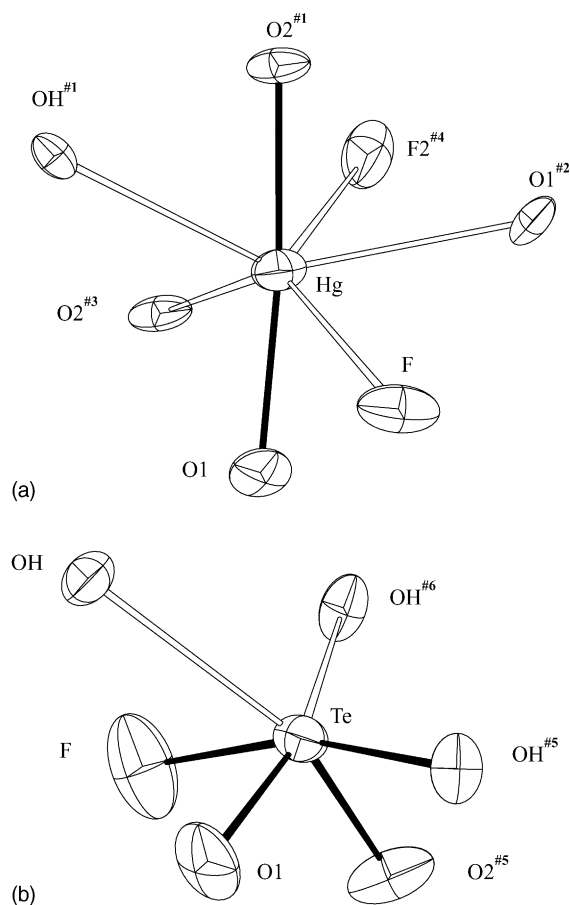


Fig. 1. Plot of the coordination around Hg (a) and Te (b), with displacement ellipsoids drawn at the 90% probability level. Short Hg–O bonds are given as solid lines, longer Hg–O bonds as well as Hg–F bonds and weak Te–OH bonds as open lines; the symmetry codes refer to Table 4.

atoms are located at considerably longer distances of about 2.65 Å. If an empirically derived bonding interaction between mercury and the corresponding ligands is considered for distances $< 3 \text{ \AA}$ [16], the coordination figure is augmented by a hydroxy group and two fluorine atoms at distances $> 2.8 \text{ \AA}$ (Fig. 1a). The observed bond length distribution is in agreement with other fluorinated oxocompounds of mercury where the Hg–O bonds are considerably shorter than the Hg–F bonds [17]. The polyhedron around mercury as a whole is extremely distorted and difficult to derive in terms of a simple geometric description like for other (undistorted) hepta-coordinate atoms (e.g. a pentagonal bipyramid or a monocapped prism). The tellurium atom is surrounded by six coordination partners (two oxygen atoms, one fluorine atom and three hydroxy groups) with bond lengths ranging from 1.88 to 3.0 Å in a highly distorted octahedron (Fig. 1b). As a matter of fact, only four of these atoms with distances $< 2.10 \text{ \AA}$ contribute significantly to the electrostatic valence around the tellurium atom (Table 5). Then the corresponding coordination figure can be described as a truncated trigonal bipyramid $\text{TeO}_2\text{F}(\text{OH})E$

with the lone-pair E located at one equatorial corner of the polyhedron. This stereochemical behaviour is quite characteristic for the Te^{IV} atom and has been described in detail for various tellurates(IV) and related compounds [18,19]. Both oxidic atoms O1 and O2 show the shortest Te–O distances of ca. 1.88 Å (and also the shortest Hg–O distances). The fluorine atom and the hydroxy group are located at considerably longer distances of 1.987(4) and 2.051(6) Å, respectively. In all fluorinated oxo- or hydroxotellurates(IV) mentioned above, there is no general tendency with respect to the atom type X (O, OH, F) and the Te– X bond length, since in some of these compounds the shortest bond is a Te–O bond, a Te–F bond or even a Te–OH bond. In the corresponding structures this scatter is caused by the different bonding interactions of these atoms to the additional coordination partners (covalent bond, intra- or intermolecular hydrogen bond etc.). The bond-valence analysis of HgTeO_2FOH (Table 5) clearly demonstrates the presence of F and OH in the structure. Although a reliable assignment of these atoms is hampered by the very similar scattering factors of the F and O atoms, and to compound matters that on the basis of the present X-ray data no location of the proton was possible, refinements of the occupancies support the present tentative model. The reliability factors were somewhat higher when F and O were interchanged ($R = 0.0196$, $wR = 0.0440$) or refined using a model of statistical disorder ($R = 0.0214$, $wR = 0.0459$).

Each $[\text{Hg}^{\text{II}}\text{O}_4\text{F}_2\text{OH}]$ polyhedron shares an edge (O1–O2) and (O2'–O1') with a long and a short Hg–O distance to constitute infinite zig-zag chains extending parallel to the $[001]$ direction. Adjacent chains are connected by interstitial Te atoms parallel to $[100]$ (Fig. 2) which results in a layered assembly parallel to (010) . The lone-pairs E of the Te^{IV} atoms are stereochemically active and are arranged oppositely to each other. Like in many other tellurites(IV) [20] or Te(IV) fluorinated compounds [21], the lone-pairs point towards

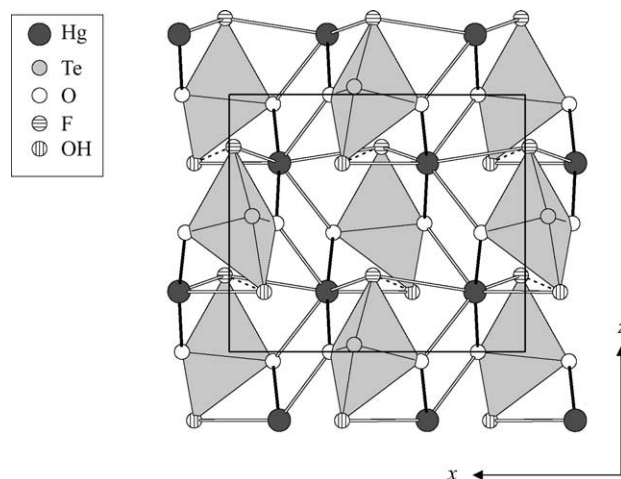


Fig. 2. Projection of the crystal structure along $[010]$; the unit cell is outlined. The TeO_2FOH anion is plotted in the polyhedral representation; interpolyhedral $\text{F} \cdots \text{OH}$ interactions are given as dotted lines.

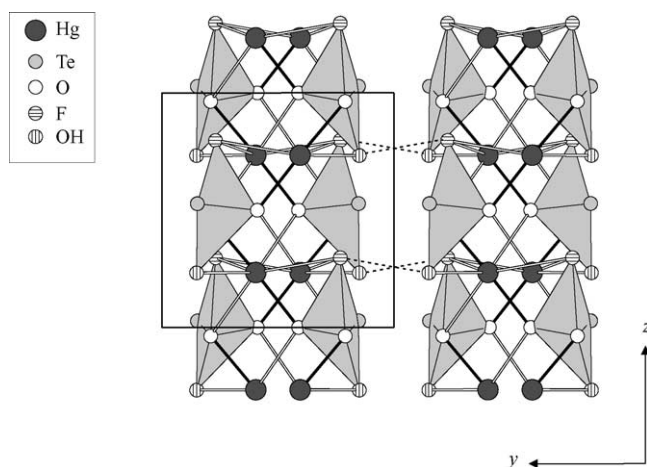


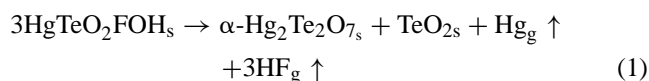
Fig. 3. Projection of the crystal structure along [100]; the unit cell is outlined. The TeO_2FOH anion is plotted in the polyhedral representation; interpolyhedral $\text{F}\cdots\text{OH}$ interactions are given as dotted lines.

the cavities of the structure, in this case to the inter-sheet spaces. Two neighbouring layers are connected perpendicular to each other only by weak $\text{F}\cdots\text{OH}$ interactions at a distance of 2.82 \AA (Fig. 3), which explains consistently the plate-like habit and the easy cleavage of the crystals.

An empirically derived correlation between the OH stretching frequencies and $\text{O}\cdots\text{O}$ distances has been reported for various OH bearing minerals and synthetic compounds [22]. On the simplified assumption that this correlation also holds for OH stretching frequencies and the corresponding $\text{F}\cdots\text{O}$ interactions, the distance $d(\text{F}-\text{O}) = 2.823(6) \text{ \AA}$ correlates with a calculated stretching frequency of $\nu(\text{OH})_{\text{calc}} = 3430 \text{ cm}^{-1}$ which is in very good agreement with the observed value of $\nu(\text{OH})_{\text{obs}} = 3440 \text{ cm}^{-1}$ (powder specimen in a KBr matrix).

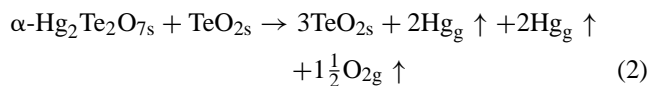
Although held together only by weak $\text{F}\cdots\text{OH}$ interactions, the crystals are comparatively stable up to ca. 300°C . The thermal decomposition proceeds in a two-step mechanism (Fig. 4) and might be formulated by the idealized reaction Eqs. (1) and (2), showing a good agreement between observed and theoretical mass losses. The first step involves a redox-reaction under formation of $\alpha\text{-Hg}_2\text{Te}_2\text{O}_7$ [1] which is accompanied by an endothermal DSC effect at ca. 455°C . Subsequent XRPD analysis of material heated up to 480°C revealed the mixed-valent $\text{Te}^{\text{IV}/\text{VI}}$ compound as the main phase besides traces of $\text{Hg}_2^{\text{II}}\text{Te}^{\text{VI}}\text{O}_5$ [2]. TeO_2 was not detected by this method, indicating that this phase is X-ray amorphous at that temperature. In the second step the remaining mercury phases decompose completely above 620°C under formation of paratellurite, $\alpha\text{-TeO}_2$, which was determined by XRPD as the only phase present.

First step:



Mass loss 22.5%, theory 21.9%

Second step:



Mass loss referring to the second step: 49.1%, theory 51.6%

Overall reaction:



Mass loss 62.7%, theory 59.7%

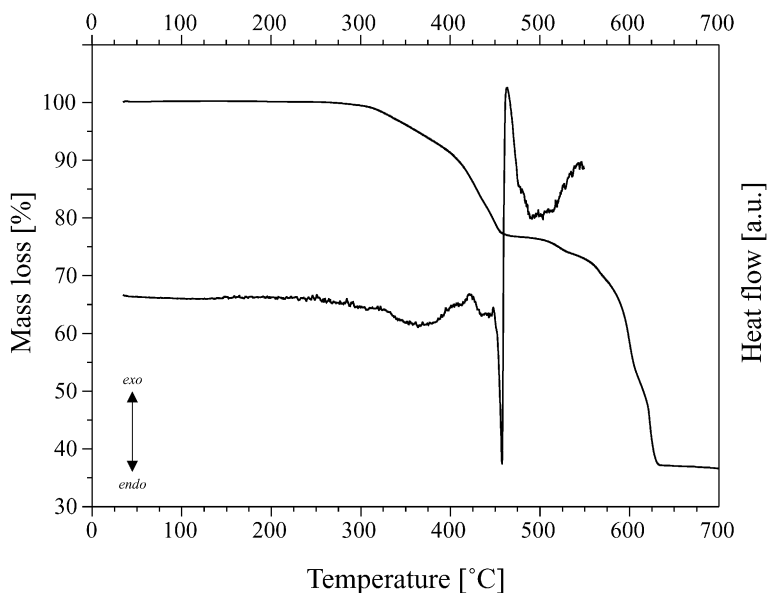


Fig. 4. TG and DSC curves of the thermal decomposition of HgTeO_2FOH .

4. Conclusion

HgTeO₂FOH has been synthesized and its structure determined by means of single crystal X-ray diffraction data.

Upon heating above 300 °C, the compound decomposes in a two-step mechanism to form paratellurite, TeO₂, with α-Hg₂Te₂O₇ (main phase) and Hg₂TeO₅ (traces) as intermediate products.

The structure is made up from distorted [Hg^{II}O₄F₂OH] polyhedra and (Te^{IV}O₂FOH)²⁻ anions as the main building units which form a layered assembly parallel to (0 1 0). Adjacent layers are connected only via F...OH interactions at a distance of 2.823(6) Å which is in agreement with IR spectroscopic data.

Neutron diffraction experiments planned for the future are considered to yield a reliable location of the proton position and to achieve a more detailed understanding of the inter- and intrapolyhedral hydrogen bonding.

Acknowledgements

I thank Dr. E. Halwax for valuable comments to improve the manuscript.

References

- [1] M. Weil, Z. Kristallogr. 218 (2003) 691–698.
- [2] M. Weil, Z. Anorg. Allg. Chem. 629 (2003) 653–657.
- [3] W. Herrendorf, HABITUS, Program for Optimization of the Crystal Shape for the Numerical Absorption Correction, Universities of Karlsruhe and Gießen, Germany, 1993–1997.
- [4] G.M. Sheldrick, SHELX97, Programs for Crystal Structure Solution and Refinement, University of Göttingen, Germany, 1997.
- [5] A.K. Spek, PLATON, a multipurpose crystallographic tool, Utrecht University, Utrecht, The Netherlands, 2001.
- [6] H.D. Flack, G. Bernardinelli, Acta Crystallogr. A55 (1999) 908–915.
- [7] I. D. Brown, The Chemical Bond in Inorganic Chemistry, Oxford University Press, 2002.
- [8] N.E. Brese, M. O’Keeffe, Acta Cryst. B47 (1991) 192–197.
- [9] E. Dowty, ATOMS for Windows, Version 5.1, Shape Software, 521 Hidden Valley Road, Kingsport, TN 37663, USA, 2000.
- [10] J.C. Jumas, M. Maurin, E. Philippot, J. Fluorine Chem. 8 (1976) 329–340.
- [11] Yu.E. Gorbunova, S.A. Linde, V.I. Pakhomov, Yu.V. Kokunov, Yu.A. Buslaev, Koord. Khim. 8 (1982) 389–395.
- [12] Yu.E. Gorbunova, S.A. Linde, V.I. Pakhomov, V.A. Sarin, N.N. Bydanov, Yu.V. Kokunov, M.P. Gustyakova, Yu.A. Buslaev, Koord. Khim. 11 (1985) 270–276.
- [13] Yu.E. Gorbunova, S.A. Linde, V.I. Pakhomov, Yu.V. Kokunov, M.P. Gustyakova, Yu.A. Buslaev, Koord. Khim. 9 (1983) 524–535.
- [14] A. Ider, J.P. Laval, B. Frit, J. Carre, J.P. Bastide, J. Solid State Chem. 123 (1996) 68–72.
- [15] L. Guillet, A. Ider, J.P. Laval, B. Frit, J. Fluorine Chem. 93 (1999) 33–38.
- [16] D. Grdenić, Quart. Rev. Chem. Soc. 19 (1965) 303–328.
- [17] M. Weil, Acta Cryst. C58 (2002) i37–i39.
- [18] J. Zemmann, Monatsh. Chem. 102 (1971) 1209–1216.
- [19] J. Galy, G. Meunier, S. Andersson, A. Åström, J. Solid State Chem. 13 (1975) 142–159.
- [20] V.A. Dolgikh, Russ. J. Inorg. Chem. (Eng. Trans.) 36 (1991) 1117–1129.
- [21] L. Guillet, J.P. Laval, B. Frit, J. Fluorine Chem. 107 (2001) 223–228.
- [22] E. Libowitzky, Monatsh. Chem. 130 (1999) 1047–1059.